

Article

Comparison of CrN, AlN and TiN Diffusion Barriers on the Interdiffusion and Oxidation Behaviors of Ni+CrAlYSiN Nanocomposite Coatings

Lijuan Zhu ^{1,2}, Chun Feng ^{1,*}, Shenglong Zhu ^{2,*}, Fuhui Wang ², Juntao Yuan ^{1,2} and Peng Wang ¹

¹ State Key Laboratory for Performance and Structural Safety of Petroleum Tubular Goods and Equipment Materials, Tubular Goods Research Institute of China National Petroleum Corporation, No. 89 Jinyeer Road, Xi'an 710077, China; zhulijuan1986@cnpc.com.cn (L.Z.); Yuanjt@cnpc.com.cn (J.Y.); wangpeng008@cnpc.com.cn (P.W.)

² Institute of Metal Research, Chinese Academy of Sciences, No. 72 Wenhua Road, Shenyang 110016, China; fhwang@mail.neu.edu.cn

* Correspondence: fengchun003@cnpc.com.cn (C.F.); slzhu@imr.ac.cn (S.Z.)

Abstract: CrN, AlN, TiN layer were prepared as diffusion barriers between the K417 substrate and Ni+CrAlYSiN nano composite coatings via vacuum arc evaporation. Oxidation kinetics and microstructure evaluation of these nano coating systems at 1000 °C after 100 h were studied. Results show that the AlN layer showed good thermodynamic stability, effectively inhibited the interdiffusion between the coating and the substrate, improved the oxidation resistance of Ni+CrAlYSiN nano composite coatings, and a single-layer Al₂O₃ film was formed on the coating. The CrN layer was decomposed, which did not block the diffusion of elements and had little effect on the oxidation resistance of the Ni+CrAlYSiN nano composite coating. The TiN layer effectively prevented the interdiffusion between the coating and the substrate. However, it deteriorated the oxidation resistance of the composite coating. Similar to the Ni+CrAlYSiN coating without a diffusion barrier, a double-layer oxide film structure with Al₂O₃ as the inner layer and Ni(Al,Cr)₂O₄ as the outer layer formed on the Ni+CrAlYSiN nano composite coatings with the CrN or TiN diffusion barrier.

Keywords: oxidation; nano; diffusion barrier; K417; interdiffusion



Citation: Zhu, L.; Feng, C.; Zhu, S.; Wang, F.; Yuan, J.; Wang, P. Comparison of CrN, AlN and TiN Diffusion Barriers on the Interdiffusion and Oxidation Behaviors of Ni+CrAlYSiN Nanocomposite Coatings. *Crystals* **2021**, *11*, 1333. <https://doi.org/10.3390/cryst11111333>

Academic Editors: Shujun Zhang and Arcady Zhukov

Received: 14 October 2021
Accepted: 29 October 2021
Published: 31 October 2021

Publisher's Note: MDPI stays neutral with regard to jurisdictional claims in published maps and institutional affiliations.



Copyright: © 2021 by the authors. Licensee MDPI, Basel, Switzerland. This article is an open access article distributed under the terms and conditions of the Creative Commons Attribution (CC BY) license (<https://creativecommons.org/licenses/by/4.0/>).

1. Introduction

High temperature protective coatings, such as MCrAlY (M is Ni, Co or NiCo) coatings, with outstanding high-temperature oxidation resistance, have been widely used to protect gas turbine components [1–5]. The content of Al in the temperature protective coating must be high enough to form a protective Al₂O₃ film and maintain its growth [6–8], due to the long-time exposure to the high-temperature environment. Considering the oxidation, corrosion resistance and consumption life of Al and Cr, the contents of Al and Cr should be increased as much as possible, but they are also subject to the embrittlement of MCrAlY coatings. According to the comprehensive requirements of oxidation resistance, heat corrosion resistance and coating plasticity, the Al content should range from 6 wt.% to 12 wt.%. There are two consumption modes of the beneficial elements Al and Cr in high temperature protective coatings. One is the outward diffusion oxidation of Al and Cr to form a protective oxide film and maintain its growth [9–12]. The other is the diffusion of Al and Cr into the substrate, which reduces the content of beneficial elements in the coating and affects the service life of the coating [13–15].

Since interdiffusion is one of the key factors affecting the service life of coatings, a diffusion barrier was introduced between the coating and substrate [16,17]. The basic requirements of a diffusion barrier between the coating and substrate [16] are as follows: (1) Low diffusion coefficient of elements in the diffusion barrier; (2) No reaction between the coating and substrate with the diffusion barrier; (3) Good thermodynamic stability of

the diffusion barrier at service temperature; (4) Good adhesion between diffusion barrier with the substrate and coating; (5) Low thermal stress at the interface between the substrate and coating. However, it is difficult to find a diffusion barrier that meets all the above conditions. Therefore, when the first condition is met, the diffusion barriers, such as TiN [18], CrN [19], Al₂O₃ [20], Al–O–N [21] or Cr₂O₃ [22], are selected by appropriately choosing other conditions.

In our previous work, a Ni+CrAlYSiN nano composite coating was prepared with high hardness, good wear resistance [23], good oxidation resistance [24] and thermal corrosion resistance [25], and the AlN diffusion barrier was introduced to effectively inhibit the interdiffusion between the coating and the substrate. It is well known that the Gibbs free energies of CrN, AlN and TiN are -198.38 kJ/mol, -378.95 kJ/mol and -416.78 kJ/mol, respectively [26]. It is not clear whether TiN is more suitable for the diffusion barrier between Ni+CrAlYSiN nano composite coating and substrate. It has not been studied whether the TiN or AlN diffusion barrier can be formed in situ when a thin layer is deposited between the Ni+CrAlYSiN nanocomposite coating and substrate. Therefore, in the present work, TiN, CrN and AlN diffusion barriers were prepared, and the effects of the above diffusion barriers on the interdiffusion and oxidation behavior of K417/Ni+CrAlYSiN nano composite coating system were discussed.

2. Materials and Methods

2.1. Sample Preparation

Nickel-base superalloy, K417 (nominal composition: 8.5–9.5 wt.% Cr, 14.0–16.0 wt.% Co, 4.8–5.7 wt.% Al, 4.5–5.0 wt.% Ti, 2.5–3.5 wt.% Mo, 0.60–0.90 wt.% V, minor C, balanced Ni) was used as the substrate alloy. Specimens of approximate dimensions $20 \times 10 \times 2.5$ mm were ground to 2000-grit SiC paper and polished with diamond paste (1.5 μ m), then ultrasonically cleaned within ethanol and acetone for 20 min. The AlN, TiN, CrN and Ni+CrAlYSiN nano composite coatings were prepared by vacuum arc evaporation. The chemical compositions of the cathode targets were Ni-21Cr-10Al-0.5Si-0.5Y (wt.%), Cr, Al and Ti with purity of 99.99 wt.%, and typical deposition parameters are given in Table 1. During the coating deposition, the argon–nitrogen mixture with a total pressure of 0.2 Pa was introduced, and the reactive gas (N₂, 99.99%) and inert gas (Ar, 99.99%) were introduced into the chamber using two independent mass-flow controllers. The detailed preparation process was described in our previous work [24]. Some specimens were coated with thick Ni+CrAlYSiN coatings only, while other specimens were coated with a CrN, AlN, or TiN thin film and then a Ni+CrAlYSiN coating via serial depositions using Cr, Al or Ti and then NiCrAlYSi targets, respectively. In order to avoid droplets that are commonly observed in the coatings deposited by vacuum arc evaporation, the CrN, AlN, and TiN thin films were prepared by filtered vacuum arc evaporation.

Table 1. Typical deposition parameters.

	Arc-Voltage (V)	Arc Current (A)	Bias Voltage (V)	Bias Duty (%)	Temperature (°C)
CrN layer	19	70	−600	20	195–215
AlN layer	30	70	−500	20	195–215
TiN layer	19	70	−600	20	195–215
Ni+CrAlYSiN coating	19	70	−300	20	195–215

2.2. Oxidation Test

Cyclic oxidation tests of the specimens, uncoated K417, K417coated with the composite coatings only, and K417 coated with the diffusion barrier layer and a composite coating, were conducted in static air in a muffle furnace for 5 cycles. In each cycle, the specimens were exposed at 1000 °C for 20 h, taken out from the furnace, cooled down at room temperature, and then weighed using an electronic balance with sensitivity of 10^{-5} g.

2.3. Characterization

Surface and cross-sectional morphologies were observed using a field-emission scanning electron microscope (SEM, Inspect F50, FEI Co., Hillsboro, OR, USA) equipped with an energy dispersive X-ray spectrometer (EDAX, X-Max, Oxford Instruments Co., Oxford, UK). To observe surface morphology, a second electron (SE) mode was adopted, while the back-scattered electron (BSE) mode was utilized to characterize cross-sectional morphologies of coating samples. The microstructures of the as-prepared diffusion barrier layers and the oxide scales were identified by X-ray diffraction (XRD), the reference codes of phases were checked from JCPDS. An electroless-nickel layer was applied on the surface of the cross-section specimens to prevent TGO (thermally-grown oxide) scales from spalling off in the specimen preparation process.

3. Results

3.1. Coating Morphology and Microstructures

Figure 1 shows the initial cross-sectional morphologies and elements depth profile of K417/CrN/Ni+CrAlYSiN and K417/TiN/Ni+CrAlYSiN. There are grey phases mainly along with a few bright phases and dark voids in the Ni+CrAlYSiN nano coatings, consistent with our previous results [24]. The grey phases comprised mainly γ -Ni, fcc-AlN and fcc-CrN with average size less than 30 nm [24]. The bright phases contained nanocrystalline solid solution γ -Ni (CrAlYSi) [23]. The almost un-nitride γ -Ni(CrAlYSi) was the splashed micro-droplet formed during vacuum arc evaporation. CrN, and TiN barrier layers, shown as thick dark lines in Figure 1, are about 300 nm and 500 nm thick, respectively. The barrier layer was quite smooth as it was prepared by filtered vacuum arc vacuum arc evaporation. According to the EDX results, the atom ratio of Cr:N, and Ti:N of the barrier layers were about 1:1. K417/Ni+CrAlYSiN and K417/AlN/Ni+CrAlYSiN samples were also prepared for the comparative study. The thickness of the AlN diffusion barrier is about 400 nm.

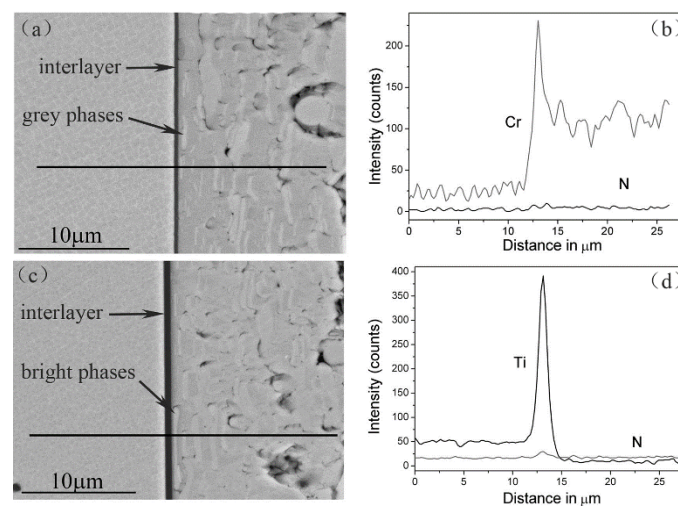


Figure 1. Cross-sectional BSE images (a,c) and elements depth profile (c,d) analyzed by EDX of the as-deposited K417/CrN/Ni+CrAlYSiN (a,b) and K417/TiN/Ni+CrAlYSiN (c,d) nano composite coating systems.

XRD analysis results showed that the structures of the three diffusion barriers are fcc-CrN and fcc-TiN with rock salt structure, hcp-AlN with braze zinc structure (Figure 2), and their reference codes are 11-0065, 38-1420 and 25-1133 from JCPDS, respectively. In addition, the CrN diffusion barrier contains a small amount of Cr₂N (35-0803).

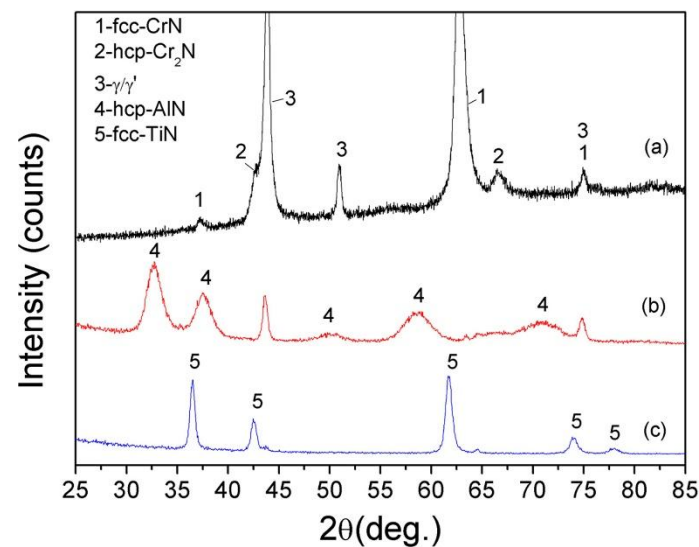


Figure 2. XRD patterns of as-deposited (a) CrN, (b) AlN and (c) TiN film.

3.2. Corrosion Kinetics and Corrosion Products

Oxidation kinetics curves of K417 with and without coatings in air at 1000 °C after 100 h are shown in Figure 3. The coated specimens with a CrN barrier layer exhibited oxidation rates slightly higher than those without the barrier layer, while the coated specimens with an AlN barrier layer exhibited oxidation rates slightly lower than those without the barrier layer. The coated specimens with a TiN barrier layer exhibited oxidation rates slightly lower at the initial stage and then slightly higher than those with CrN barrier layer. Slight mass loss of the coated specimens with a TiN barrier layer after 80 h, was detected, suggesting scale spallation occurrence on the surface. The mass gains of the K417/Ni+CrAlYSiN, K417/CrN/Ni+CrAlYSiN, K417/AlN/Ni+CrAlYSiN and K417/TiN/Ni+CrAlYSiN coating systems after 100 h were 0.45, 0.51, 0.28 and 0.46 mg/cm², respectively. That is, the nanocomposite coating with an AlN barrier layer exhibited the lowest oxidation rates.

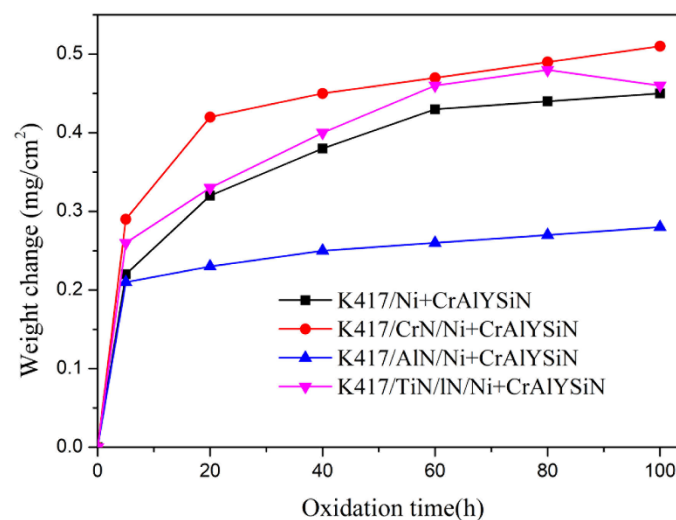


Figure 3. Corrosion kinetics of the composite coating with or without a diffusion barrier after 100 h oxidation at 1000 °C in static air.

XRD patterns of the surfaces of specimens after 100 h oxidation test are displayed in Figure 4. The TGO scales on the nanocomposite coatings without an AlN diffusion barrier were composed of α -Al₂O₃ (50-1496) and Ni(Al,Cr)₂O₄ (23-1272) (Figure 4a), those on the

nanocomposite coatings with a CrN or TiN diffusion barrier were composed of Cr_2O_3 (38-1479), $\alpha\text{-Al}_2\text{O}_3$ and $\text{Ni}(\text{Al,Cr})_2\text{O}_4$ (Figure 4b,d), while those on the nanocomposite coatings with an AlN diffusion barrier were exclusively alpha-alumina (Figure 4c). For the nanocomposite coatings, Cr_7Ni_3 (51-0637) was detected on the specimens without a diffusion barrier (Figure 4a), while CrN was detected on those with the AlN and TiN barrier layer (Figure 4c,d).

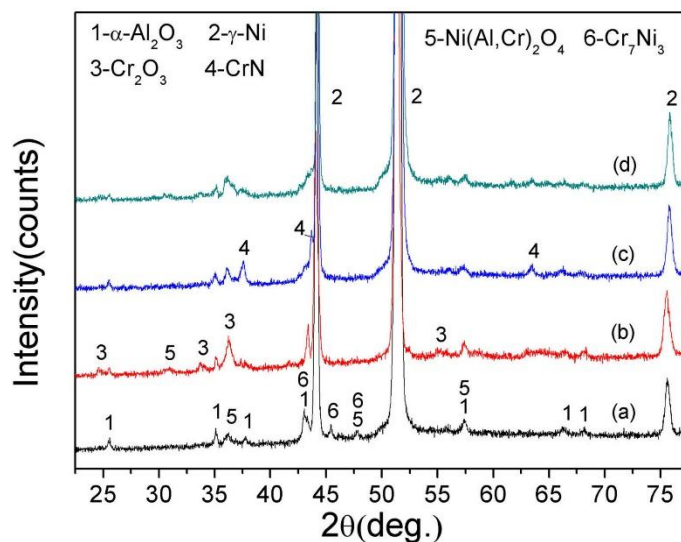


Figure 4. XRD patterns of (a) K417/Ni+CrAlYSiN, (b) K417/CrN/Ni+CrAlYSiN, (c) K417/AlN/Ni+CrAlYSiN and (d) K417/TiN/Ni+CrAlYSiN coating systems after 100 h oxidation at 1000 °C in air.

3.3. Characterization by SEM and EDS

The morphologies and the element depth profiles of the K417/Ni+CrAlYSiN coating system after oxidation at 1000 °C for 100 h were shown in Figure 5. The oxidation and interdiffusion behavior of the K417/Ni+CrAlYSiN coating system is generally consistent with our previous investigation [24,25]. Neither cracking nor spallation of the TGO was detected on the nanocomposite coatings (Figure 5a). A TGO scale about 2.6 μm was formed on the surface (Figure 5b). Combined with the results analyzed by XRD, the cross-section image demonstrates that a double-layered dense oxide scale, inner Al_2O_3 layer and outer $\text{Ni}(\text{Al,Cr})_2\text{O}_4$ layer, formed on K417/Ni+CrAlYSiN coating system (Figure 5b). Within the composite coating, many dark hcp-AlN circles and particles were observed. Congregated hcp-AlN particles were also observed near the coating/substrate interface. Interdiffusion between the coating and the substrate was obvious. Many granular and even needle-like TiN phases were formed in the interdiffusion zone. Diffusion of N from the coating into the substrate and Co from the substrate into the coating was most evident (Figure 5c).

The morphologies and the element depth profiles of the K417/CrN/Ni+CrAlYSiN coating system after oxidation at 1000 °C for 100 h were shown in Figure 6. Large-sized particles were formed on the surface of the composite coatings (Figure 6a); however, neither cracking nor spallation of the TGO was detected. A thermally-grown oxide (TGO) scale about 2.9 μm was formed on the surface (Figure 6b). Combined with the results analyzed by XRD, the cross-section image demonstrates that a double-layered dense oxide scale, inner Al_2O_3 layer and outer mixture layer mainly dominated by $\text{Ni}(\text{Al,Cr})_2\text{O}_4$, formed on K417/CrN/Ni+CrAlYSiN coating system (Figure 6b). Similar to the K417/Ni+CrAlYSiN coating system, hcp-AlN particles were formed within the composite coating. However, no large-sized hcp-AlN particles near the coating/substrate interface were observed. The CrN diffusion barrier disappeared. Interdiffusion between the coating and the substrate was obvious. Many TiN particles were formed in the interdiffusion zone. Diffusion of N and Cr from the coating into the substrate, Co from the substrate into the coating was most evident (Figure 6c).

In contrast, no such interdiffusion zone was observed on K417/AlN/Ni+CrAlYSiN (Figure 7) and K417/TiN/Ni+CrAlYSiN coating systems (Figure 8). The ©/©' microstructure beneath the AlN and TiN barrier layers remained unchanged, the AlN and TiN diffusion barrier layer kept continuous and dense (Figures 7b and 8b). However, the thickness of the diffusion barrier for the K417/TiN/Ni+CrAlYSiN coating system was changed from 0.5 μm to 1.1 μm with a triple-layered structure after oxidation at 1000 $^{\circ}\text{C}$ for 100 h. The center layer was rich in Ti and N, outer layer near the substrate was rich in Al, Ti and N, while outer layer near the coating was rich in Cr, Ti and N. Again, the phenomenon of AlN congregation within the coatings of K417/TiN/Ni+CrAlYSiN coating system occurred. However, the size of AlN particles was quite smaller than that in the K417/Ni+CrAlYSiN and K417/CrN/Ni+CrAlYSiN coating systems. A unique alumina scale about 1.6 μm was formed on the surface of K417/AlN/Ni+CrAlYSiN coating systems (Figure 7b) and neither cracking nor spallation of the TGO was detected (Figure 7b). In contrast, a double-layered dense oxide scale, inner Al_2O_3 layer and outer mixture layer mainly dominated by $\text{Ni}(\text{Al,Cr})_2\text{O}_4$, was formed on K417/TiN/Ni+CrAlYSiN coating system (Figure 8b). The thickness of the oxide scale on K417/TiN/Ni+CrAlYSiN coating system ranged from about 2 μm to more than 7 μm in the bulged oxide zone (Figure 8b).

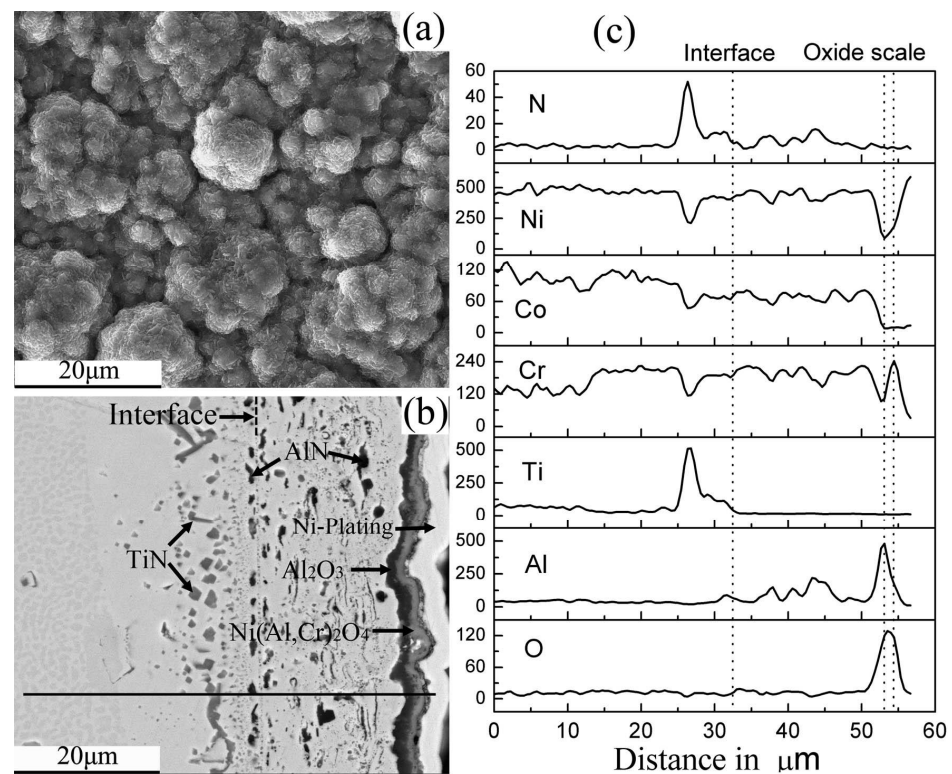


Figure 5. Surface SEM image (a), Cross-sectional BSE image (b) and the element depth profiles ((c), analyzed by EDX) of K417/Ni+CrAlYSiN coating system after oxidation for 100 h at 1000 $^{\circ}\text{C}$ in air.

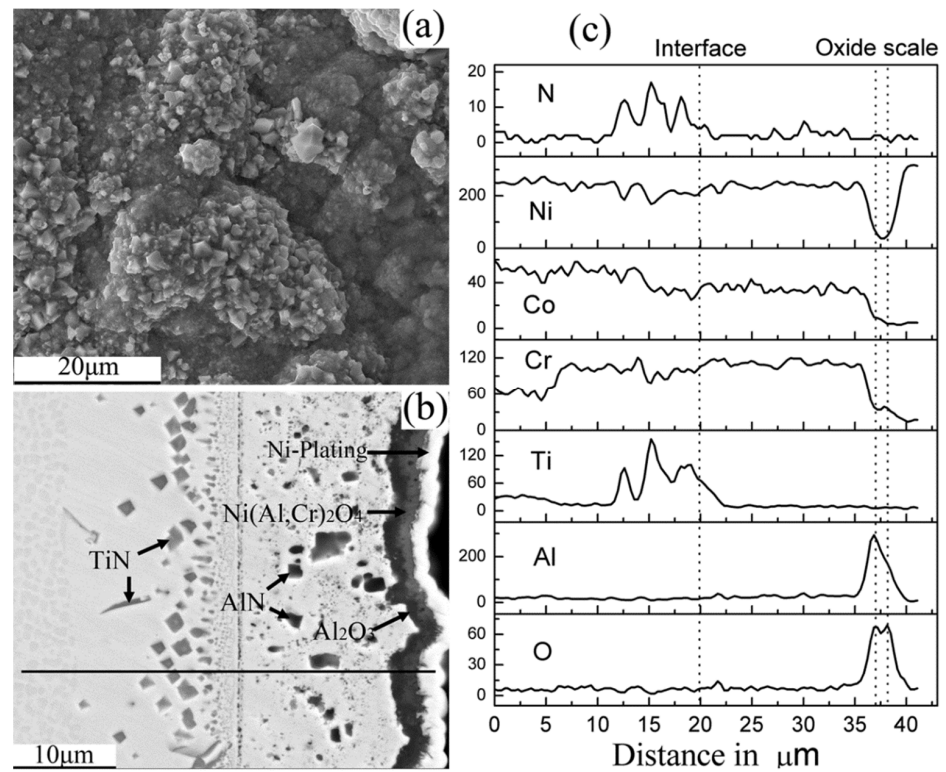


Figure 6. Surface SEM image (a), Cross-sectional BSE image (b) and the element depth profiles (c), analyzed by EDX of K417/ CrN/Ni+CrAlYSiN coating system after oxidation for 100 h at 1000 °C in air.

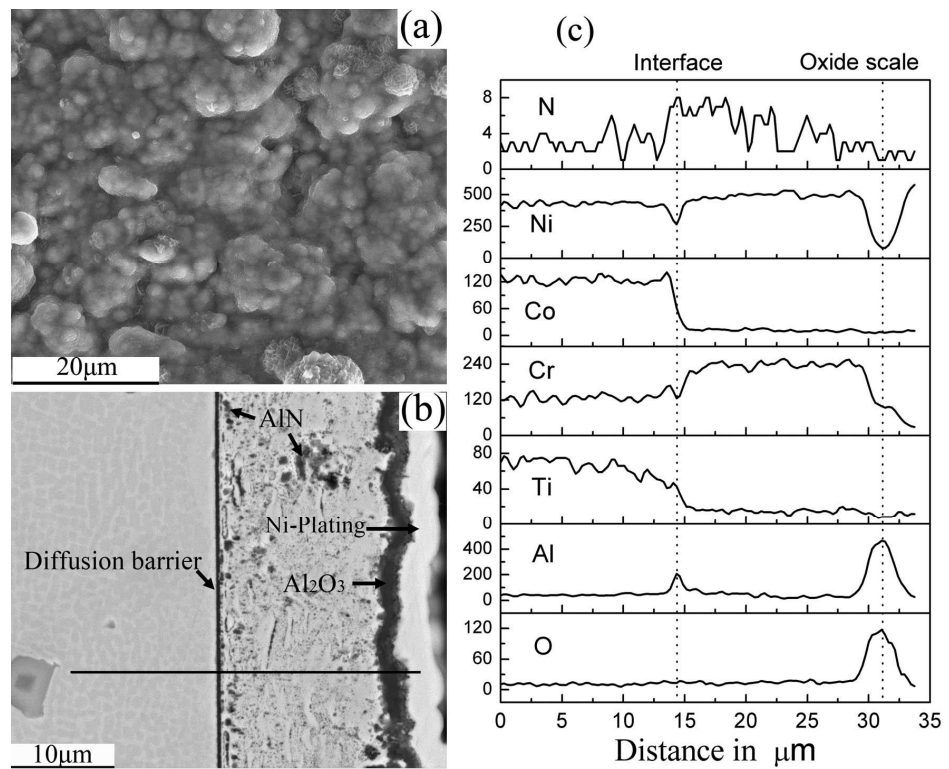


Figure 7. Surface SEM image (a), Cross-sectional BSE image (b) and the element depth profiles (c), analyzed by EDX of K417/ AlN/Ni+CrAlYSiN coating system after oxidation for 100 h at 1000 °C in air.

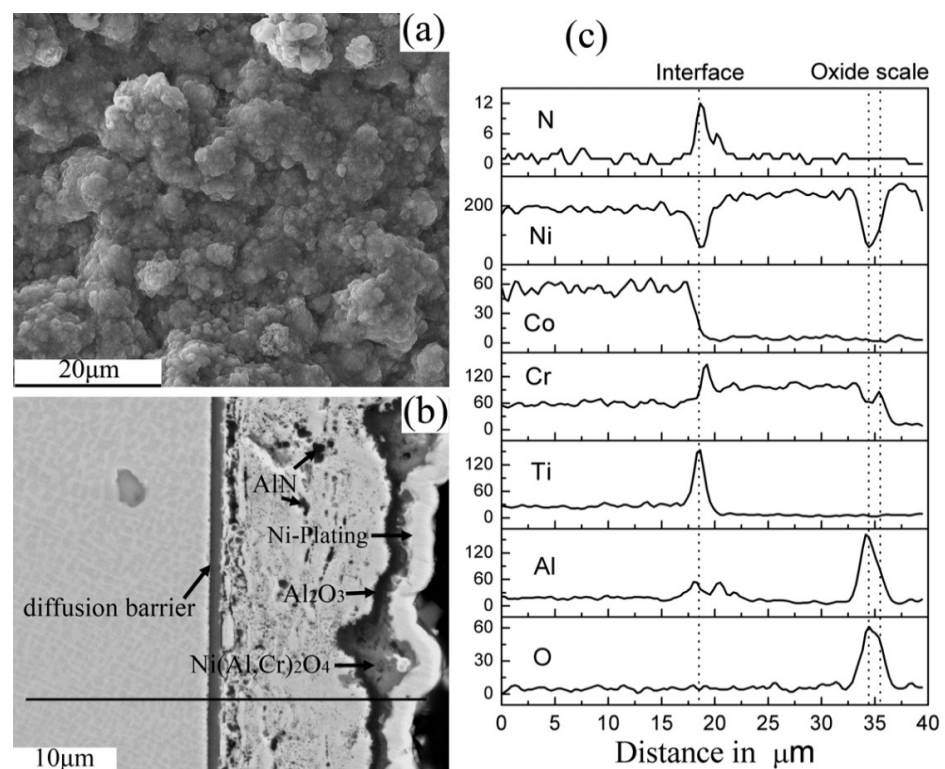


Figure 8. Surface SEM image (a), Cross-sectional BSE image (b) and the element depth profiles (c), analyzed by EDX of K417/TiN/Ni+CrAlYSiN coating system after oxidation for 100 h at 1000 °C in air.

4. Discussion

4.1. Influence of Diffusion Barrier on Interdiffusion

As is abundantly clear, the interdiffusion between the coating and the substrate will reduce the service life of the coating. Therefore, many compounds, such as TiN [18], CrN [19,27], Al₂O₃ [20,28], Al–O–N [21,29] or Cr₂O₃ [22], are used as diffusion barriers between MCrAlY coatings and superalloys.

In this study, CrN, AlN and TiN nitride were introduced as the diffusion barrier between the K417 matrix and Ni+CrAlYSiN composite coating. The standard formation of Gibbs free energies for each nitride phase at 1000 °C is −198.38 kJ/mol for CrN, −378.95 kJ/mol for AlN and −416.78 kJ/mol for TiN [26]. Therefore, from the perspective of thermodynamics, TiN diffusion barrier is the most stable.

The K417 substrate contains elements Ti, Al and Cr, Ni+CrAlYSiN composite coating contains elements Al and Cr. Therefore, for the K417/CrN/Ni+CrAlYSiN sample, the following reactions occurred near the interface between the substrate and coating:



Therefore, during the oxidation process, the CrN diffusion barrier was decomposed and granular and needle TiN was formed in the interdiffusion region.

If only from the perspective of thermodynamics, the TiN diffusion barrier should be more stable than the AlN diffusion barrier. The AlN diffusion barrier will eventually degenerate to TiN. However, after the K417/TiN/Ni+CrAlYSiN sample was oxidized at 1000 °C for 100 h, a Cr rich nitride layer was formed near the coating side of the TiN diffusion barrier, and an Al rich nitride layer was formed near the substrate side. Therefore, the thickness of the nitride layer at the coating/substrate interface changes from 500 nm as

deposited to 1.1 μm . In contrast, the AlN diffusion barrier is very stable after oxidation at 1000 $^{\circ}\text{C}$ for 100 h.

Research shows that TiN is an ionic compound with FCC rock salt structure [26]. In general, the defect concentration of ionic compounds is relatively high. It can be seen from the Ti-N phase diagram that there are many compounds in TiN, such as Ti_2N , Ti_3N , etc. When the content of Al is less than 57%, the (Ti, Al) N can maintain the FCC rock salt structure. The Ti-Al-N ternary phase diagram [30] shows that there are two ternary phases Ti_3AlN and Ti_2AlN at 1000 $^{\circ}\text{C}$. The crystal structures of TiN phase and CrN phase are completely consistent. In addition, the lattice constants of TiN phase and CrN phase are 0.4242 nm and 0.4148 nm, respectively, which are relatively close. Therefore, the positions of metal atoms in TiN phase and CrN phase can be replaced with each other to form (Ti, Cr)N films in the form of alloys. Therefore, when there are elements such as Al and Cr near the TiN diffusion barrier, the solid soluble Al and Cr in TiN can be transformed into TiCrAlN composite layer.

According to the element content in the matrix and the atomic size, from low to high content followed by Ti, Al and Cr, and from small to large size followed by Al, Cr, and Ti, respectively. Therefore, it is probable that the diffusion rate of Al in the matrix to the substrate and diffusion barrier interface is bigger than that of Ti and Cr, resulting in the formation of Al rich Ti nitride layer near the substrate side of TiN diffusion barrier. The content of Cr in the coating is higher than Al, and AlN is more stable than CrN. Therefore, a Cr rich nitride layer containing Ti was formed near the coating side of the TiN diffusion barrier. Due to the diffusion of beneficial elements Cr and Al from the coating to the interface where TiN is located, the effective content of Cr element in the coating was reduced, resulting in the formation of nodular oxide with large thickness on the surface of the coating and the peeling of the oxide film. Therefore, although TiN effectively prevented the interdiffusion between the coating and the substrate, it deteriorated the oxidation resistance of the composite coating. The structural transformation of TiN diffusion barrier in the oxidation process needs to be further studied. It should be pointed out that because the Ni content in the Ni+CrAlYSiN composite coating is equivalent to that in the matrix, it is impossible to judge whether TiN can prevent the diffusion of nickel in the present work. However, Cheng et al. [31] found that the TiN diffusion barrier could not prevent the Ni diffusion from the NiCrAlY coating into TiAl substrate during the oxidation experiment at 1000 $^{\circ}\text{C}$.

The standard formation Gibbs free energies of AlN and TiN at 1000 $^{\circ}\text{C}$ are -378.95 kJ/mol and -416.78 kJ/mol [26], respectively, and the driving force of the second reaction formula theoretically is -37.83 kJ/mol. However, the AlN diffusion barrier is HCP braze zinc structure with covalent bonding, while TiN diffusion barrier is FCC rock salt structure with ionic bonding. Therefore, the second reaction formula is not a simple displacement reaction, but also involves the transformation of crystal structure, which probably increases the activation energy required for the second reaction. The conversion of hcp-AlN to fcc-AlN can be completed at a high pressure of 12 Gpa. As described in our previous work [24], there is no non stoichiometric AlN_x . hcp-AlN with braze zinc structure is a broadband semiconductor with band gap width of 6.2 eV. hcp-AlN is covalently bonded, and the defect concentration in covalently bonded semiconductors is several orders of magnitude lower than that in ionic crystals [32]. In fact, the point defects in hcp-AlN are almost negligible [33]. Therefore, the AlN diffusion barrier with HCP braze zinc structure can remain stable and effectively inhibit the mutual diffusion between the coating and the substrate.

4.2. Influence of Diffusion Barrier on Growth of Oxide Scale

In our previous work [24], the results showed that the K417 substrate suffered catastrophic corrosion after oxidation at 1000 $^{\circ}\text{C}$ for 100 h, and the Ni+CrAlYSiN composite coating greatly improved the oxidation resistance of the K417 substrate. In the present work, the experimental results show that the weight gain of K417/Ni+CrAlYSiN, K417/

CrN/Ni+CrAlYSiN, K417/AlN/Ni+CrAlYSiN and K417/TiN/Ni+CrAlYSiN coating systems after oxidation for 100 h is 0.45, 0.51, 0.28 and 0.46 mg/cm², respectively. The decomposition of the CrN diffusion barrier has little effect on the oxidation resistance of the Ni+CrAlYSiN composite coating, and the oxidation weight gain increases slightly. The AlN diffusion barrier is very stable in the oxidation process, which effectively inhibits the interdiffusion between the coating and the substrate. A single layer α -Al₂O₃ film is formed on the coating surface, and the oxidation weight gain of the coating is reduced by about 50 percent. Therefore, the application of the AlN diffusion barrier significantly improves the oxidation resistance of Ni+CrAlYSiN composite coatings. After the TiN diffusion barrier is applied, the initial oxidation weight gain of the composite coating is smaller than that of the composite coating with the CrN diffusion barrier, and the oxidation weight gain is the same when it is oxidized to 60 h. However, after 80 h of oxidation, the composite coating with the TiN diffusion barrier showed a slight weight loss due to the peeling of oxide on the coating surface. The TiN diffusion barrier is relatively stable in the oxidation process, and effectively inhibits the mutual diffusion between the coating and the substrate. However, due to the enrichment of Al and Cr in the coating, the formation of nodular oxide with large thickness on the surface of the coating and the peeling of the oxide film occurred. Therefore, although the TiN diffusion barrier effectively prevented the interdiffusion between the coating and the substrate, it deteriorated the oxidation resistance of the composite coating.

5. Conclusions

CrN, AlN, TiN were prepared as diffusion barriers between the K417 substrate and Ni+CrAlYSiN composite coating via vacuum arc evaporation. Oxidation kinetics, microstructure evaluation and oxidation performance of these coating systems at 1000 °C after 100 h were investigated, and the following conclusions can be drawn:

1. The CrN diffusion barrier decomposed, which did not block the diffusion of elements and had little effect on the oxidation resistance of Ni+CrAlYSiN composite coating. Similar to the Ni+CrAlYSiN coating without a diffusion barrier, a double-layer oxide film structure with Al₂O₃ as the inner layer and Ni(Al,Cr)₂O₄ as the outer layer formed on the coating.
2. The AlN diffusion barrier showed good thermodynamic stability, effectively inhibited the interdiffusion between the coating and the substrate, and a single-layer Al₂O₃ film was formed on the coating. The AlN diffusion barrier significantly improved the oxidation resistance of Ni+CrAlYSiN composite coating.
3. The TiN diffusion barrier effectively prevented the interdiffusion between the coating and the substrate. However, it deteriorated the oxidation resistance of the composite coating. Similar to the Ni+CrAlYSiN coating without diffusion barrier, a double-layer oxide film structure with Al₂O₃ as the inner layer and Ni(Al,Cr)₂O₄ as the outer layer formed on the coating.

Author Contributions: Conceptualization, L.Z.; investigation, L.Z. and S.Z.; data curation, L.Z., C.F. and J.Y.; writing—original draft preparation, L.Z.; writing—review and editing, C.F. and P.W.; supervision, S.Z. and F.W.; project administration, L.Z. All authors have read and agreed to the published version of the manuscript.

Funding: This project is financially supported by the Youth Science and Technology Nova Plan of Shaanxi Province (No. 2020KJXX-064), the National Natural Science Foundation of China (NO. 51804335), Major science and technology projects of Inner Mongolia Autonomous Region (No. 2020ZD0019), and the CNPC Science and Technology Development Project (No. 2019E-25-05 and No. 2020B-4020).

Institutional Review Board Statement: We choose to exclude this statement because the study did not involve humans or animals.

Informed Consent Statement: We choose to exclude this statement because the study did not involve humans or animals.

Data Availability Statement: Data sharing not applicable.

Acknowledgments: The authors wish to acknowledge the Youth Science and Technology Nova Plan of Shaanxi Province (No. 2020KJXX-064), and the financial support by the National Natural Science Foundation of China (No. 51804335), Major science and technology projects of Inner Mongolia Autonomous Region (No. 2020ZD0019), and the CNPC Science and Technology Development Project (No. 2019E-25-05 and No. 2020B-4020).

Conflicts of Interest: The authors declare no conflict of interest.

References

1. Nicholls, J.R.; Simms, N.J.; Chan, W.Y.; Evans, H.E. Smart overlay coatings-concept and practice. *Surf. Coat. Technol.* **2002**, *149*, 236–244. [[CrossRef](#)]
2. Goward, G.W. Progress in coatings for gas turbine airfoils. *Surf. Coat. Technol.* **1998**, *108–109*, 73–79. [[CrossRef](#)]
3. Podchernyaeva, I.A.; Panasyuk, A.D.; Teplenko, M.A.; Podol'ski, V.I. Protective Coatings on Heat-resistant Nickel Alloys (Review). *Powder Metall. Met. Ceram.* **2000**, *39*, 434–444. [[CrossRef](#)]
4. Pomeroy, M.J. Coatings for gas turbine materials and long term stability issues. *Mater. Des.* **2005**, *26*, 223–231. [[CrossRef](#)]
5. Wang, J.L.; Chen, M.H.; Yang, L.L.; Sun, W.Y.; Zhu, S.L.; Wang, F.H. Nanocrystalline coatings on superalloys against high temperature oxidation and corrosion: A review. *Corros. Com.* **2021**, *1*, 58–69. [[CrossRef](#)]
6. Yang, S.S.; Yang, L.L.; Chen, M.H.; Wang, J.L.; Zhu, S.L.; Wang, F.H. Understanding of failure mechanisms of the oxide scales formed on nanocrystalline coatings with different Al content during cyclic oxidation. *Acta Mater.* **2021**, *205*, 116576. [[CrossRef](#)]
7. Brandl, W.; Toma, D.; Grabke, H.J. The characteristics of alumina scales formed on HVOF-sprayed MCrAlY coatings. *Surf. Coat. Technol.* **1998**, *108*, 10–15.
8. Godlewski, K.; Godlewska, E. The effect of chromium on the corrosion resistance of aluminide coatings on nickel and nickel-based substrates. *Mater. Sci. Eng.* **1987**, *88*, 103–109. [[CrossRef](#)]
9. Johnson, J.B.; Nicholls, J.R.; Hurst, R.C.; Hancock, P. The Mechanical Properties of Surface Scales on Nickel-Base Superalloys-II. Contaminant Corrosion. *Corros. Sci.* **1978**, *18*, 543–553. [[CrossRef](#)]
10. Ren, X.; Wang, F.H.; Wang, X. High-temperature oxidation and hot corrosion behaviors of the NiCr–CrAl coating on a nickel-based superalloy. *Surf. Coat. Technol.* **2005**, *198*, 425–431. [[CrossRef](#)]
11. Chen, G.F.; Lou, H.Y. Oxidation behavior of sputtered Ni-3Cr-20Al nanocrystalline coating. *Mater. Sci. Eng. A* **1999**, *271*, 360–365. [[CrossRef](#)]
12. Ren, X.; Wang, F.H. High-temperature oxidation and hot-corrosion behavior of a sputtered NiCrAlY coating with and without aluminizing. *Surf. Coat. Technol.* **2006**, *201*, 30–37. [[CrossRef](#)]
13. Zhang, K.; Wang, Q.M.; Sun, C.; Wang, F.H. Preparation and oxidation behavior of NiCrAlYSi coating on a cobalt-base superalloy K40S. *Corros. Sci.* **2008**, *50*, 1707–1715. [[CrossRef](#)]
14. Knotek, O.; Lugscheider, E.; Löffler, F.; Beele, W. Diffusion barrier coatings with active bonding, designed for gas turbine blades. *Surf. Coat. Technol.* **1994**, *68*, 22–26. [[CrossRef](#)]
15. Lang, F.Q.; Narita, T. Improvement in oxidation resistance of a Ni3Al-based superalloy IC6 by rhenium-based diffusion barrier coatings. *Intermetallics* **2007**, *15*, 599–606. [[CrossRef](#)]
16. Nicolet, M. Diffusion barrier in thin films. *Thin Solid Films* **1978**, *52*, 415–443. [[CrossRef](#)]
17. Müller, J.; Schierling, M.; Zimmermann, E.; Neuschütz, D. Chemical vapor deposition of smooth α -Al₂O₃ films on nickel base superalloys as diffusion barriers. *Surf. Coat. Technol.* **1999**, *120*, 16–21. [[CrossRef](#)]
18. Lou, H.; Wang, F. Effect of Ta, Ti and TiN barriers on diffusion and oxidation kinetics of sputtered CoCrAlY coatings. *Vacuum* **1992**, *43*, 757–761. [[CrossRef](#)]
19. Li, W.Z.; Wang, Q.M.; Gong, J.; Sun, C.; Jiang, X. Interdiffusion reaction in the CrN interlayer in the NiCrAlY/CrN/DSM11 system during thermal treatment. *Appl. Surf. Sci.* **2009**, *255*, 8190–8193. [[CrossRef](#)]
20. Wang, Q.M.; Zhang, K.; Gong, J.; Cui, Y.Y.; Sun, C.; Wen, L.S. NiCoCrAlY coatings with and without an Al₂O₃/Al interlayer on an orthorhombic Ti₂AlNb-based alloy: Oxidation and interdiffusion behaviors. *Acta Mater.* **2007**, *55*, 1427–1439. [[CrossRef](#)]
21. Wang, Q.M.; Wu, Y.N.; Guo, M.H.; Ke, P.L.; Gong, J.; Sun, C.; Wen, L.S. Ion-plated Al-O-N and Cr-O-N films on Ni-base superalloys as diffusion barriers. *Surf. Coat. Technol.* **2005**, *197*, 68–76. [[CrossRef](#)]
22. Cheng, Y.X.; Wang, W.; Zhu, S.L.; Xin, L.; Wang, F.H. Arc ion plated-Cr₂O₃ intermediate film as a diffusion barrier between NiCrAlY and γ -TiAl. *Intermetallics* **2010**, *18*, 736–739. [[CrossRef](#)]
23. Zhu, L.J.; Zhu, S.L.; Wang, F.H. Effects of bias voltage and nitrogen flow rate on the structure and properties of Ni+CrAlYSiN nanocrystalline composite coatings. *Chin. J. Mater. Res.* **2013**, *27*, 53–59. (In Chinese)
24. Zhu, L.J.; Zhu, S.L.; Wang, F.H. Preparation and oxidation behavior of nanocrystalline Ni+CrAlYSiN composite coating with AlN diffusion barrier on Ni-based superalloy K417. *Corros. Sci.* **2012**, *60*, 265–274. [[CrossRef](#)]
25. Zhu, L.J.; Zhu, S.L.; Wang, F.H. Hot corrosion behavior of a Ni+CrAlYSiN composite coating in Na₂SO₄–25 wt.% NaCl melt. *Appl. Surf. Sci.* **2013**, *268*, 103–110. [[CrossRef](#)]
26. Liang, Y.J.; Che, M.C. *Handbook of Thermodynamic Data for Inorganic Compounds*, 1st ed.; Northeast University Press: Shenyang, China, 1993. (In Chinese)

27. Li, W.Z.; Yao, Y.; Wang, Q.M.; Bao, Z.B.; Gong, J.; Sun, C.; Jiang, X. Improvement of oxidation-resistance of NiCrAlY coatings by application of CrN or CrON interlayer. *J. Mater. Res.* **2008**, *23*, 341–352. [[CrossRef](#)]
28. Müller, J.; Neuschütz, D. Efficiency of α -alumina as diffusion barrier between bond coat and bulk material of gas turbine blades. *Vacuum* **2003**, *71*, 247–251. [[CrossRef](#)]
29. Cremer, R.; Witthaut, M.; Reichert, K.; Schierling, M.; Neuschütz, D. Thermal stability of Al-O-N PVD diffusion barriers. *Surf. Coat. Technol.* **1998**, *108*, 48–58. [[CrossRef](#)]
30. Zhang, J.; Zhao, Y.H. *Multi Arc Ion Plating Technology and Application*; Metallurgical Industry Press: Beijing, China, 2007; p. 90. (In Chinese)
31. Cheng, Y.X. Investigation on the Diffusion Barrier of γ -TiAl/NiCrAlY Coating Systems. Ph.D. Thesis, Institute of Metal Research, Chinese Academy of Sciences, Shenyang, China, 2009. (In Chinese)
32. Mehrer, H. *Diffusion in Solids: Fundamentals, Methods, Materials, Diffusion-Controlled Processes*; Springer Series in Solid-State Sciences; Springer: Berlin/Heidelberg, Germany, 2007; Volume 155.
33. Chen, H.Y.; Stock, H.R.; Mayr, P. Plasma-assisted nitriding of aluminum. *Surf. Coat. Technol.* **1994**, *64*, 139–147. [[CrossRef](#)]